T-shaped waveguides for quantum-wire intersubband lasers

Thomas Herrle, Stefan Schmult, Markus Pindl, Ulrich T. Schwarz, and Werner Wegscheider
Institut für Experimentelle und Angewandte Physik, Universität Regensburg, 93040 Regensburg, Germany
(Received 5 January 2005; revised manuscript received 19 April 2005; published 8 July 2005)

We present a T-shaped waveguide for a quantum-wire intersubband laser in the GaAs/AlGaAs heterosystem for the midinfrared spectral region around 8 μm. Such a device is fabricated using the cleaved edge overgrowth (CEO) technique. The suggested waveguide structure is compatible to this growth technique. The confinement factor and the waveguide losses due to free carrier absorption are calculated solving the scalar wave equation and compared to the results for a conventional quantum cascade laser (QCL) in the GaAs/AlGaAs material system based on coupled quantum-wells. We show that the optical mode can be confined near the active region of a quantum-wire cascade structure with the presented T-shaped waveguide design. Simultaneously the waveguide losses can be reduced compared to a conventional QCL waveguide design. However, the confinement factor is substantially reduced as a result of a small optically active region in the quantum-wire cascade device.

DOI: 10.1103/PhysRevB.72.035316 PACS number(s): 42.55.Px, 42.60.By, 42.60.Da

I. INTRODUCTION

Since their realization in 1994[1] quantum cascade lasers (QCL) have matured as compact coherent light sources in the midinfrared spectral region enabling important advances in areas such as ultrahigh resolution spectroscopy, ultrahigh sensitivity gas sensing, and optical communications. One of many milestones was the presentation of a QCL in the GaAs/AlGaAs heterosystem in 1998.[2] Recently, also terahertz quantum cascade lasers have been demonstrated.[3] Despite significant improvements such as room-temperature continuous wave operation[4] and high-temperature pulsed operation,[5] quantum cascade lasers exhibit high threshold current densities mainly due to short nonradiative intersubband lifetimes. Basic theoretical considerations predict a decrease of these nonradiative losses in lower dimensional systems[6–8] due to the reduction of electron-longitudinal-optical-phonon (LO-phonon) scattering, which represents a fast parallel decay channel in competition with the photon emission. Since the underlying basic principle of a quantum cascade emitter does not depend on the dimensionality of the charge carrier system, emission and population inversion could be achieved not only in conventional coupled quantum-well systems but also in coupled quantum-wire or even quantum-dot systems. Experiments on quantum-dot systems[9,10] and quantum-wire systems[11] have been published recently. In this work we will focus on the quantum-wire system of Ref. 11. This quantum-wire intersubband emitter device shows midinfrared emission at a peak wavenumber of 1200 cm^{-1} and was realized using the cleaved edge overgrowth (CEO) technique,[12] which has been already successfully employed for optically and electrically pumped interband quantum-wire lasers in the nearinfrared spectral region.[13,14] In these latter works a T-shaped waveguide was used to provide feedback in this structure. In this work we will present a T-shaped waveguide compatible to the cleaved edge overgrowth technique to confine the optical mode close to the active region and thus to achieve laser activity in a quantum-wire intersubband emitter structure in the midinfrared spectral region.

II. INVESTIGATED SAMPLE STRUCTURE

Waveguide calculations solving the scalar wave equation have been performed to conceive a suitable waveguide structure for the quantum-wire cascade structure of Ref. 11. The investigated structure is shown in Fig. 1. In a first growth step, a GaAs/$Al_{0.33}Ga_{0.67}As$ quantum cascade structure is grown along the [001]-crystal direction on a highly doped GaAs n^+ substrate ($n_{Si}=3\times10^{18}$ cm^{-3}). The active region along the [001] direction in the presented waveguide calculations is simulated by a 1.6562 μm $Al_{0.16}Ga_{0.84}As$ layer with an effective refractive index of $n_{eff}=3.22$. However, in contrast to the QCL structure by Sirtori *et al.* based on quantum-well transitions,[15] the active region is left undoped and is surrounded on each side by 3.5 μm intrinsic GaAs for waveguide purposes along the [001] direction. At the top and bottom heavily doped 1 μm thick n^{++}-GaAs layers ($n_{Si}=6\times10^{18}$ cm^{-3}) are grown. This heterostructure is cleaved *in situ* within the MBE chamber across the nonpolar (110)-

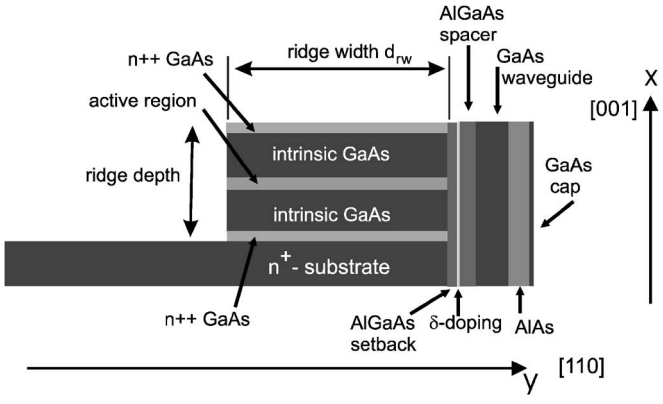

FIG. 1. Sample structure of the quantum-wire cascade structure considered for the presented waveguide calculations. This structure is realized employing the cleaved edge overgrowth (CEO) technique (Ref. 12). The relevant crystal directions are given. The extension of the quantum wires is normal to the drawing plane. The sketch is not to scale.

surface and overgrown along the [110]-crystal direction. The [110]-growth sequence starts with a 500 Å thick $Al_{0.33}Ga_{0.67}As$ setback layer. Charge carriers are supplied via a remote δ-silicon doping. Calculations predict the formation of wirelike states at the cleavage plane which are confined to this area within about 200 Å.[8] The [110]-growth sequence is continued by a 3000 Å $Al_{0.33}Ga_{0.67}As$ spacer layer. In contrast to Ref. 11 we add an intrinsic GaAs layer to guide the optical mode along the [110] direction. In this work we will discuss the influence of the thickness of this layer on some waveguide properties, as confinement factor and waveguide losses of the optical mode. The [110]-growth sequence in our proposal of a waveguide structure ends with a 0.7 μm AlAs layer with low refractive index to limit the optical mode towards the sample surface and a 200 Å GaAs cap layer. The waveguide calculations have been performed using different ridge widths d_{rw} of the first growth step and the ridge was assumed to be rectangular shaped with a depth down to the n^+ substrate, as indicated in Fig. 1. The ridge is introduced to restrict the area of numerical calculation. Furthermore such ridge structures are defined to laterally confine the optical mode, as it is done in conventional QCL structures. The optical modes in our quantum-wire cascade structure are calculated by solving the scalar wave equation[16]

$$\frac{\partial^2\psi}{\partial x^2}+\frac{\partial^2\psi}{\partial y^2}+\frac{\partial^2\psi}{\partial z^2}+n^2(x,y)\left(\frac{2\pi}{\lambda}\right)^2\psi=0. \tag{1}$$

The refractive index $n(x,y)$ is a function of x and y, where x is along the first growth direction ([001] direction) and y along the second growth direction ([110] direction). We use the scalar wave equation, since it turned out that a transfer matrix calculation combined with the use of an effective refractive index is not appropriate for our problem. We expect to introduce only a small error by using the scalar approximation instead of the vectorial calculation which would be too time-consuming. A general solution of the scalar wave equation can be written in the form

$$\psi=e^{-i\beta z}\sum_{\mu=1}^{N_x}\sum_{\nu=1}^{N_y}c_{\mu\nu}\phi_{\mu\nu}(x,y). \tag{2}$$

The wave propagates along the z direction with the propagation constant β. The functions

$$\phi_{\mu\nu}(x,y)=\sqrt{\frac{4}{L_xL_y}}\sin\left(\frac{\pi}{L_x}\mu x\right)\sin\left(\frac{\pi}{L_y}\nu y\right) \tag{3}$$

form a complete orthogonal set. For a numerical solution one is restricted to a finite basis $N_x\times N_y$, whereas for an exact solution N_x and N_y have to go to infinity. L_x and L_y are the dimensions of the area of the calculation in x and y direction. Substituting ψ in the wave equation (1) by Eq. (2), one obtains a system of algebraic equations:

$$\sum_{\mu=1}^{N_x}\sum_{\nu=1}^{N_y}A_{\mu'\nu',\mu\nu}c_{\mu\nu}=\left[\left(\frac{\beta\lambda}{2\pi}\right)^2-n_0^2\right]c_{\mu'\nu'}, \tag{4}$$

where β is the propagation constant of the guided mode, λ the emission wavelength and n_0 some constant value, which is introduced for computational convenience. The coefficients $A_{\mu'\nu',\mu\nu}$ are given by

$$A_{\mu'\nu',\mu\nu}=\int_0^{L_x}dx\int_0^{L_y}dy\{[n^2(x,y)-n_0^2]\phi_{\mu'\nu'}(x,y)\phi_{\mu\nu}(x,y)\}-\frac{\lambda^2}{4}\left(\frac{\mu^2}{L_x^2}+\frac{\nu^2}{L_y^2}\right)\delta_{\mu'\mu}\delta_{\nu'\nu}. \tag{5}$$

After an index conversion, Eq. (4) becomes an eigenvalue equation

$$\hat{A}\vec{C}=\Lambda\vec{C}. \tag{6}$$

The eigenvalues Λ are given by

$$\Lambda=\left(\frac{\beta\lambda}{2\pi}\right)^2-n_0^2. \tag{7}$$

From these eigenvalues one is able to deduce the propagation constant of the guided modes β, and from the eigenvectors $\vec{C}$ the corresponding modes can be calculated via Eq. (2).

The refractive index $n(x,y)=n_{real}(x,y)+iK(x,y)$ is complex. The real part n_{real} of the refractive index is derived from the classical Drude model:

$$n_{real}(\omega,n_d)=n_\infty\left(1-\frac{\omega_p^2}{\omega^2}\right)^{1/2}, \tag{8}$$

where $\omega=2\pi c/\lambda$, and $\omega_p=(n_de^2/\epsilon_0n_\infty^2m^*)^{1/2}$ is the plasma frequency. n_d is the n-type bulk doping concentration of the layers, m^* is the effective mass of the electrons in the layer, and n_∞ is the high frequency refractive index. The imaginary part of the refractive index K is given by

$$K=\frac{n_de^3\lambda^3}{16\pi^3c^3\epsilon_0n_\infty}\frac{1}{m^{*2}\mu_e}, \tag{9}$$

where μ_e is the electron mobility in the corresponding layers. From the imaginary part K of the complex refractive index one is able to derive the loss $\alpha=(4\pi/\lambda)K$ due to free carrier absorption in the different layers. In Table I, the real part of the complex refractive index and the loss α of the different layers along the [001] direction are given. We also applied our numerical scheme to the QCL structure by Sirtori *et al.*[15] to compare our results to those given in Ref. 15 and to the results for the quantum-wire structure. Therefore we also listed the values for the real part of the refractive index and the loss α we used for the calculations of the structure by Sirtori *et al.* In Table II, we present the real part of the refractive index and the loss α for the layers along the [110] direction.

III. RESULTS OF WAVEGUIDE CALCULATIONS

In Fig. 2 we present the fundamental modes and a first order mode (upper left contour plot) of the quantum-wire cascade structure of Fig. 1 for several GaAs waveguide layer thicknesses d_{wg} and a ridge width of $d_{rw}=30$ μm. The calculations were performed for a wavelength of $\lambda=8.3$ μm corresponding to a wave number of about 1200 cm^{-1} as given in

TABLE I. Real part of the complex refractive index and loss α of the layers along the first growth step ([001] direction) of the quantum-wire cascade structure. The two 3.5 μm thick GaAs layers and the 1.6562 μm thick active region along the [001] direction are undoped for the quantum-wire cascade structure (upper numbers), whereas in the QCL structure by Sirtori *et al.* (Ref. 15) they are doped (lower numbers).

Layer thickness	Layer material	n_{real}	α (cm^{-1})
1 μm	n^{++}-GaAs	2.31	1740
	($n_{Si}=6\times10^{18}$ cm^{-3})		
3.5 μm	intrinsic GaAs	3.3	0.015
	($n_{Si}=4\times10^{16}$ cm^{-3})	3.29	1.8
	(Ref. 15)		
1.6562 μm	$Al_{0.16}Ga_{0.84}As$	3.22	0.018
	($n_{Si}=8.6\times10^{16}$ cm^{-3})	3.21	15.4
	(Ref. 15)		
3.5 μm	intrinsic GaAs	3.3	0.015
	($n_{Si}=4\times10^{16}$ cm^{-3})	3.29	1.8
	(Ref. 15)		
1 μm	n^{++}-GaAs	2.31	1740
	($n_{Si}=6\times10^{18}$ cm^{-3})		
10 μm	n^{+}-GaAs substrate	2.85	574
	($n_{Si}=3\times10^{18}$ cm^{-3})		

Ref. 11. We also present the corresponding calculated confinement factors Γ of the optical modes, which represent the fraction of the mode that overlaps the optically active region of the quantum-wire cascade structure (see also Fig. 3). The optically active region of the quantum-wire cascade structure extends along the 1.6562 μm thick active region of the first growth step ([001] direction) and at the cleavage plane about 200 Å along the [110] direction in the direction of the first growth step. The optically active region is very small in the quantum-wire case. This is the reason why the confinement factor is much smaller than in the quantum-well case (see Table III). It should be noted at this point, that the choice of the active region is rather arbitrary, since the presented definition of the confinement factor in the quantum wire, as well as in the quantum-well case, includes not only the alternating three coupled quantum wells, which represent the actual optically active region along the first growth step ([001] direction), but also the injector regions. While the actual value of the confinement factor is not so important, it represents an important instrument to optimize the waveguide structure. In Fig. 2 it can be seen that for small GaAs waveguide layer thicknesses the fundamental mode overlaps the first growth step to a large amount. For a GaAs waveguide layer thickness of $d_{wg}=4.5$ μm the first order mode (upper left contour plot in Fig. 2) becomes favorable compared to the fundamental mode with respect to the confinement factor and the waveguide losses (see also Fig. 3 and Fig. 4). For thicker GaAs waveguide layers the fundamental mode becomes confined at the cleavage plane, where the wirelike states reside. For even thicker GaAs waveguide layers, the fundamental mode is pulled away from the cleavage plane and becomes confined within the GaAs waveguide layer along the [110] direction. With increasing thickness of the GaAs waveguide layer the fundamental mode spreads towards the n^{+}-GaAs substrate within the GaAs waveguide layer. The reason for this spreading is the fact that the mode is not confined by a material with low refractive index in the direction towards the GaAs substrate. In the [001] direction towards the surface of the quantum-wire cascade structure, however, the mode is confined by the transition from the GaAs waveguide layer with a high refractive index ($n=3.3$) to air with a low refractive index ($n=1$). The maximum of the fundamental mode is also pulled away from the cleavage plane into the GaAs layer and towards the n^{+}-GaAs substrate with increasing thickness of this layer. The confinement factor for the fundamental mode has its maximum at a thickness of the GaAs wave-

TABLE II. Real part of the complex refractive index and loss α of the layers along the second growth step ([110] direction) of the quantum-wire cascade structure.

Layer thickness	Layer material	n_{real}	α (cm^{-1})
ridge width d_{rw}	1st growth step		
0.35 μm	$Al_{0.33}Ga_{0.67}As$	3.13	0.035
waveguide layer thickness d_{wg}	GaAs	3.3	0.015
0.7 μm	AlAs	2.86	0.15
0.02 μm	GaAs	3.3	0.015

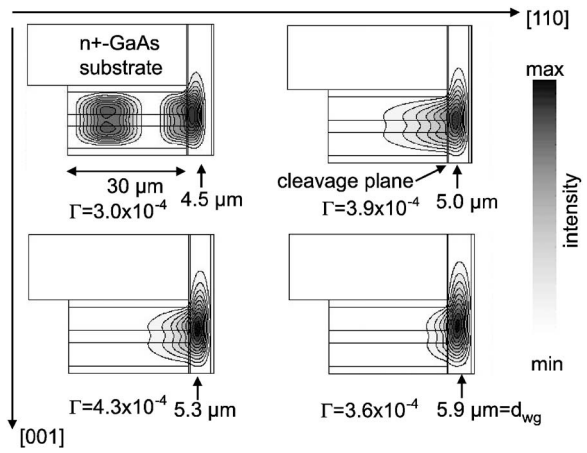

FIG. 2. Contour plots of the fundamental modes and the first order mode (upper left contour plot) of the quantum-wire cascade structure of Fig. 1 for several GaAs waveguide layer thicknesses d_{wg} and a ridge width of $d_{rw}=30$ μm. The corresponding calculated confinement factors Γ of the optical modes are also given. The confinement factor has a maximum for a thickness of the GaAs waveguide layer of about 5.3 μm (see also Fig. 3).

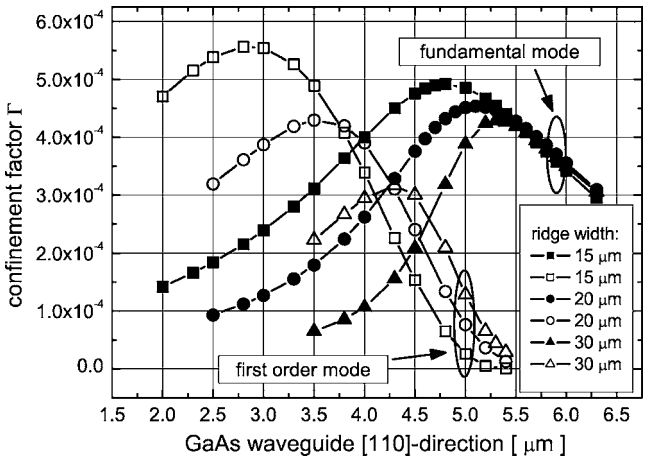

FIG. 3. Confinement factor Γ of the fundamental mode (closed symbols) in dependence of the thickness of the GaAs waveguide layer along the [110] direction for different ridge widths. For wider ridges the GaAs waveguide layer has to be thicker to achieve best confinement. For smaller GaAs waveguide layer thicknesses the first order mode (open symbols) has a better confinement factor than the corresponding fundamental mode.

guide layer of $d_{wg}=5.3$ μm for a 30 μm wide ridge.

In Table III we compare some important characteristics of the fundamental mode for the structure by Sirtori *et al.* as given in Ref. 15 and as calculated by us with the results for the quantum-wire cascade structure for a GaAs waveguide layer thickness of $d_{wg}=5.3$ μm and a ridge width of $d_{rw}=30$ μm. The values for the QCL structure by Sirtori *et al.* given in Ref. 15 were obtained using a one dimensional calculation, neglecting the additional lateral confinement by the ridge geometry. We obtained our values for the QCL structure by Sirtori *et al.* by applying our numerical scheme of a two-dimensional calculation assuming a ridge width of 30 μm. The results of our waveguide calculations for the QCL structure by Sirtori *et al.* confirm the results given in Ref. 15. Differences might be explained by the use of different refractive indices and losses of the several layers. In addition the values given in Ref. 15 are calculated for a different wavelength of $\lambda=9.4$ μm. Comparing the calculated results for the QCL structure by Sirtori *et al.* and the quantum-wire cascade structure, one can see that the waveguide losses α are reduced by about a factor of three. This is mainly due to the reduced overlap of the mode with the highly doped n^{++}-contact layers, since the mode is more drawn towards the intrinsic GaAs waveguide layer with low loss along the [110] direction. In Ref. 15 the overlap of the mode with these lossy, doped layers accounts for 90% of the total waveguide losses. Our calculations for this structure lead to about 87% of the total waveguide losses. In the quantum-wire case it is even more dramatic, since almost all the loss (about 99%) can be attributed to the overlap of the mode with these highly doped n^{++} layers. This is due to the fact that the 3.5 μm thick GaAs layers and the 1.6562 μm thick active region along the [001] direction are undoped in the quantum-wire case. The only regions that are doped in the quantum-wire case are the n^{++}-contact layers, the n^{+} substrate and the active region at the cleavage plane ($n_{Si}=8.6\times10^{16}$ cm^{-3}), which has a minor contribution to the waveguide losses.

In Fig. 4 we present the waveguide losses for the fundamental mode (closed symbols) in dependence of the GaAs waveguide layer thickness along the [110] direction for various ridge widths. The losses decrease with increasing GaAs waveguide layer thickness along the second growth direction. This is attributed to the fact that the overlap of the mode with the lossy n^{++}-contact layers decreases, since the mode is drawn towards this waveguide layer along the [110] direction. However, for an optimized waveguide structure not only the losses are important, but also the confinement factor,

TABLE III. Comparison of some characteristics of the fundamental mode for the QCL structure by Sirtori *et al.* as calculated in Ref. 15, as calculated by us, and for the quantum-wire cascade structure. For the latter structure the waveguide losses α are reduced by about a factor of 3 compared to the quantum-well system. The confinement factor and the figure of merit, however, are reduced in the quantum-wire cascade structure due to the small overlap of the mode with the optically active region.

	QCL structure [Sirtori *et al.* (Ref. 15)]	QCL structure (Sirtori *et al.*)	Quantum-wire structure
n_{real}	3.21	3.24	3.25
loss α (cm^{-1})	16	14	5.3
confinement factor Γ	0.31	0.28	4.3×10^{-4}
figure of merit Γ/α (cm)	1.9×10^{-2}	2.0×10^{-2}	8.0×10^{-5}

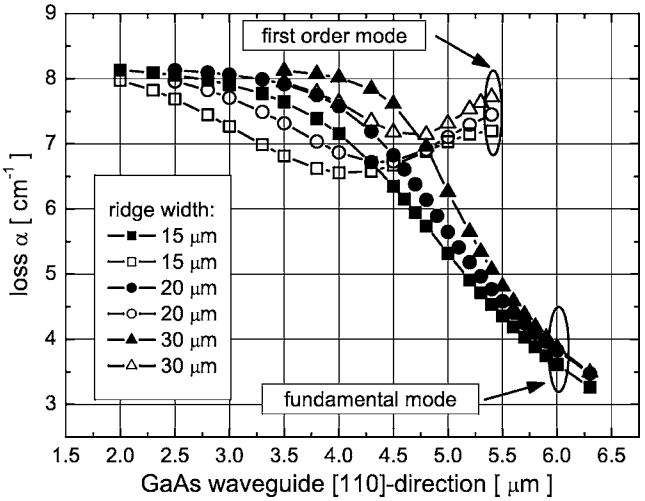

FIG. 4. Waveguide loss of the fundamental mode (closed symbols) in dependence of the thickness of the GaAs waveguide layer along the [110] direction for different ridge widths. The losses decrease with increasing GaAs waveguide layer thickness along the second growth direction, due to a decreased overlap of the fundamental mode with the lossy n^{++}-contact layers. For small GaAs waveguide layer thicknesses the first order mode (open symbols) has lower waveguide losses than the corresponding fundamental mode. The different dependence of the waveguide losses on the waveguide layer thickness along the [110] direction is explained by the splitting of the first order mode.

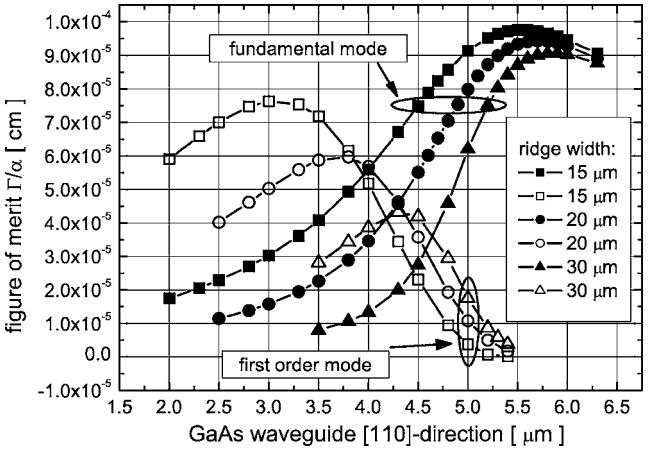

FIG. 5. Figure of merit of the fundamental mode (closed symbols) in dependence of the thickness of the GaAs waveguide layer along the [110] direction for different ridge widths. For small GaAs waveguide layer thicknesses the figure of merit of the first order mode (open symbols) is higher than the figure of merit of the corresponding fundamental mode. Because of the higher waveguide losses, the maximum value of the figure of merit for the first order mode is smaller than the maximum value for the fundamental mode for all calculated ridge widths.

which decreases with increasing GaAs waveguide layer thickness. For smaller GaAs waveguide layer thicknesses the first order mode becomes favorable compared to the fundamental mode (see upper left contour plot in Fig. 2 and Fig. 3). In addition, the waveguide losses are increased due to an increased overlap of the fundamental mode with the lossy contact layers for smaller GaAs waveguide layer thicknesses along the [110] direction. The confinement factor Γ is smaller for the quantum-wire structure than for the quantum-well structure by Sirtori *et al.*, because of the small active region with an extension of about 200 Å at the cleavage plane, as already discussed above. Consequently, also the figure of merit, which is the ratio of the confinement factor Γ and the waveguide losses α, is reduced in the quantum-wire structure by a factor of about 250 compared to the QCL structure by Sirtori *et al.* (see Table III). The figure of merit is maximized in Ref. 15 to optimize the waveguide, in order to achieve a confinement factor as high as possible with simultaneous low waveguide losses. The figure of merit for the quantum-wire structure is shown in Fig. 5 in dependence of the GaAs waveguide layer thickness along the [110] direction for different ridge widths for the fundamental as well as for the first order mode.

It is interesting to note that for small GaAs waveguide layer thicknesses the first order mode becomes favorable compared to the fundamental mode. The confinement factor for the first order mode is larger than for the fundamental mode, the waveguide loss is decreased and consequently the figure of merit is increased. The reason for that fact is that the fundamental mode has a large overlap with the first growth step of our heterostructure and is pulled away from the cleavage plane. The first order mode, however, is split into two parts. One part is concentrated in the first growth step and the second part is concentrated at the cleavage plane (upper left contour plot in Fig. 2). This second part makes the first order mode favorable compared to the fundamental mode. However, the waveguide losses for the first order mode are higher than for the fundamental mode for an optimized GaAs waveguide layer thickness, because of a large overlap of the first order mode with the first growth step and thus with the lossy n^{++}-contact layers. The waveguide losses in dependence of the GaAs waveguide layer thickness along the [110] direction show a different behavior for the first order mode compared to the fundamental mode (Fig. 4). This is due to the splitting of the first order mode. For small waveguide layer thicknesses both parts of the first order mode have a large overlap with the lossy n^{++}-contact layers and therefore the waveguide losses are high. For thicker GaAs waveguide layers the overlap with the lossy n^{++}-contact layers of the part of the first order mode, concentrated at the optically active region of the quantum-wire intersubband structure, is decreased. Therefore the waveguide losses are decreased. For even larger GaAs waveguide layer thicknesses the intensity of this part of the first order mode decreases in favor of the part, concentrated in the first growth step, which has a large overlap with the lossy n^{++}-contact layers. Consequently, the waveguide losses are increased again. The confinement factor for the first order mode has also got a maximum in dependence of the GaAs waveguide layer thickness along the [110] direction. However, this maximum occurs at smaller GaAs waveguide layer thicknesses compared to the fundamental mode (Fig. 3). At small ridge widths (d_{rw}=15 μm) the maximum confinement factor of the first order mode exceeds the maximum confinement factor of the fundamental mode. However, due to the higher

losses in the optimized region of the first order mode, the maximum value of the figure of merit for the first order mode is smaller than for the fundamental mode for all calculated ridge widths (Fig. 5).

We also performed waveguide calculations changing the thickness of the originally 3.5 μm intrinsic GaAs waveguide layers along the [001] direction. These results show that for smaller thicknesses of these waveguide layers the confinement factor is increased. However, at the same time the waveguide losses are dramatically increased, due to an increased overlap with the lossy n^{++}-contact layers, so that in the end the figure of merit is decreased. Increasing the waveguide layer thickness along the [001] direction leads to a decrease in the waveguide losses, due to a reduced overlap of the optical mode with the lossy n^{++}-contact layers. However, at the same time the confinement factor is decreased. Although the figure of merit is increased, when increasing the waveguide layer thickness along the [001] direction, this has some drawbacks. Besides the reduced confinement factor, the GaAs waveguide layer thickness along the [110] direction has to be increased to achieve an optimized waveguide. This increases the material consumption in the MBE growth. The 3.5 μm thick waveguide layers along the [001] direction represent a good compromise between waveguide losses, confinement factor and moderate waveguide layer thicknesses.

To simulate gain, we introduced a positive imaginary part of the refractive index for the active region. The value of the imaginary part of the refractive index in the active region of the quantum-wire cascade structure is chosen, so that the imaginary part of the eigenvalue of the fundamental mode becomes positive, which means to compensate the waveguide and mirror losses in the quantum-wire cascade structure. The results of these calculations show that the maximum gain is not achieved for the same GaAs waveguide layer thickness at which the figure of merit and the confinement factor have their maxima. It turns out that the maximum gain is reached for a GaAs waveguide layer thickness that is slightly higher than the value for the maximum confinement factor. For example for a ridge width of $d_{rw}=30$ μm the maximum gain is reached for a GaAs waveguide layer thickness of $d_{wg}=5.4$ μm. These results show that a high confinement factor is more important than low waveguide losses in the quantum-wire cascade structure. The calculations with a positive imaginary part of the complex refractive index, which is introduced to the active region, show that this value has to be about 250 times larger for the quantum-wire structure than for the structure by Sirtori *et al.*,[15] to achieve the same positive output gain. This is in agreement with the ratio of the figure of merit for the quantum-wire and quantum-well system. Taking into account the better inversion ratio achievable in quantum-wire systems,[8] a rough estimate predicts that the gain in the quantum-wire case is about a factor 10 smaller than in the quantum-well case. This is due to the small confinement factor in the quantum-wire case compared to the quantum-well case. This stresses the importance of increasing the confinement factor in the quantum-wire case. Nevertheless it should be possible to reach laser threshold in quantum-wire cascade structures. It is possible to increase the confinement factor, for example by replacing the GaAs waveguide layer along the [110] direction by a waveguide layer with a higher refractive index. This would also reduce the thickness of this waveguide layer needed to achieve an optimized confinement, as first calculations show. Furthermore in view of the presentation of a noncascaded intersubband laser by Gmachl *et al.*,[17] where the confinement factor is also very small ($\Gamma \approx 7.5\times10^{-3}$), reaching laser threshold in quantum-wire cascade devices seems possible.

IV. CONCLUSION

In summary, we demonstrated a T-shaped waveguide design for the midinfrared that is able to confine the optical mode close to the optically active region in a quantum-wire cascade structure. The confinement factor and the waveguide losses depend on the thickness of the GaAs waveguide layer along the second growth step. Therefore, this thickness has to be adjusted in order to optimize the waveguide properties. The waveguide losses in the quantum-wire cascade structure with a T-shaped waveguide design turn out to be reduced compared to the quantum-well structure. The presented waveguide calculations are the basis for the realization of a quantum-wire intersubband laser for the midinfrared spectral region.

ACKNOWLEDGMENT

This work is supported by the Deutsche Forschungsgemeinschaft within the framework of the Graduiertenkolleg "Nichtlinearität und Nichtgleichgewicht in kondensierter Materie" (GRK 638).

[1] J. Faist, F. Capasso, D. L. Sivco, C. Sirtori, A. L. Hutchinson, and A. Y. Cho, Science **264**, 553 (1994).

[2] C. Sirtori, P. Kruck, S. Barbieri, P. Collot, and J. Nagle, Appl. Phys. Lett. **73**, 3486 (1998).

[3] R. Köhler, A. Tredicucci, F. Beltram, H. E. Beere, E. H. Linfield, A. G. Davies, D. A. Ritchie, R. C. Iotti, and F. Rossi, Nature (London) **417**, 156 (2002).

[4] M. Beck, D. Hofstetter, T. Aellen, J. Faist, U. Oesterle, M. Ilegems, E. Gini, and H. Melchior, Science **295**, 301 (2002).

[5] N. Ulbrich, G. Scarpa, A. Sigl, J. Roßkopf, G. Böhm, G. Abstreiter, and M.-C. Amann, Electron. Lett. **37**, 1341 (2001).

[6] S. Briggs, D. Jovanovic, and J. P. Leburton, Appl. Phys. Lett. **54**, 2012 (1989).

[7] J. P. Leburton, J. Appl. Phys. **56**, 2850 (1984).

[8] I. Keck, S. Schmult, W. Wegscheider, M. Rother, and A. P. Mayer, Phys. Rev. B **67**, 125312 (2003).

[9] N. Ulbrich, J. Bauer, G. Scarpa, R. Boy, D. Schuh, G. Abstreiter, S. Schmult, and W. Wegscheider, Appl. Phys. Lett. **83**, 1530

(2003).
[10] S. Anders, L. Rebohle, F. F. Schrey, W. Schrenk, K. Unterrainer, and G. Strasser, Appl. Phys. Lett. **82**, 3862 (2003).
[11] S. Schmult, I. Keck, T. Herrle, W. Wegscheider, M. Bichler, D. Schuh, and G. Abstreiter, Appl. Phys. Lett. **83**, 1909 (2003).
[12] L. N. Pfeiffer, K. West, H. L. Störmer, J. P. Eisenstein, K. W. Baldwin, D. Gershoni, and J. Spector, Appl. Phys. Lett. **56**, 1697 (1990).
[13] W. Wegscheider, L. N. Pfeiffer, M. M. Dignam, A. Pinczuk, K. W. West, S. L. McCall, and R. Hull, Phys. Rev. Lett. **71**, 4071 (1993).
[14] W. Wegscheider, L. Pfeiffer, K. West, and R. E. Leibenguth, Appl. Phys. Lett. **65**, 2510 (1994).
[15] C. Sirtori, P. Kruck, S. Barbieri, H. Page, J. Nagle, M. Beck, J. Faist, and U. Oesterle, Appl. Phys. Lett. **75**, 3911 (1999).
[16] Dietrich Marcuse, *Theory of Dielectric Optical Waveguides*, 2nd ed. (Academic, New York, 1991).
[17] C. Gmachl, F. Capasso, A. Tredicucci, D. L. Sivco, A. L. Hutchinson, S. N. G. Chu, and A. Y. Cho, Appl. Phys. Lett. **73**, 3830 (1998).